Cite as: M. Ganji *et al.*, *Science* 10.1126/science.aar7831 (2018).

Real-time imaging of DNA loop extrusion by condensin

Mahipal Ganji,[1] Indra A. Shaltiel,[2]* Shveta Bisht,[2]* Eugene Kim,[1] Ana Kalichava,[1] Christian H. Haering,[2]† Cees Dekker[1]†

[1]Department of Bionanoscience, Kavli Institute of Nanoscience Delft, Delft University of Technology, Delft, Netherlands. [2]Cell Biology and Biophysics Unit, Structural and Computational Biology Unit, European Molecular Biology Laboratory, Heidelberg, Germany.

*These authors contributed equally to this work.

†Corresponding author. Email: christian.haering@embl.de (C.H.H.); c.dekker@tudelft.nl (C.D.)

It has been hypothesized that Structural Maintenance of Chromosomes (SMC) protein complexes such as condensin and cohesin spatially organize chromosomes by extruding DNA into large loops. Here, we provide unambiguous evidence for loop extrusion by directly visualizing the formation and processive extension of DNA loops by yeast condensin in real-time. We find that a single condensin complex is able to extrude tens of kilobase pairs of DNA at a force-dependent speed of up to 1,500 base pairs per second, using the energy of ATP hydrolysis. Condensin-induced loop extrusion is strictly asymmetric, which demonstrates that condensin anchors onto DNA and reels it in from only one side. Active DNA loop extrusion by SMC complexes may provide the universal unifying principle for genome organization.

The spatial organization of chromosomes is of paramount importance to cell biology. Members of the SMC family of protein complexes, including condensin, cohesin, and the Smc5/6 complex, play vital roles in restructuring genomes during the cellular life cycle (*1*–*3*). The principles by which SMC complexes achieve these fundamental tasks are still incompletely understood. Models based on random cross-linking of DNA by pairwise interactions or conformational changes in the DNA superhelicity have been proposed (*4*, *5*). An alternative hypothesis suggested that SMC protein complexes bind to small loops in the genome to then processively enlarge them (*6*). More recently, the idea emerged that condensin can start and subsequently extrude DNA loops, which would elegantly explain how condensin mediates the formation of mitotic chromosomes structures observed in electron micrographs and deduced from Hi-C experiments (*7*, *8*). Indeed, polymer simulations showed that loop extrusion can, in principle, result in the efficient disentanglement and compaction of chromatin fibers (*9*–*11*). The recent discovery that condensin exhibits DNA translocase activity (*12*) was consistent with, but did not provide conclusive evidence for (*13*), DNA loop extrusion.

In this Report, we visualize the formation of DNA loops by the *Saccharomyces cerevisiae* condensin complex in real time (Fig. 1A). We tethered both ends of a double-stranded 48.5-kilobase pair (kbp) λ-DNA molecule to a passivated surface (*14*, *15*), using flow to adjust the DNA end-to-end length to a distance much shorter than its contour length (Fig. 1B). We then imaged DNA after staining with Sytox Orange (SxO; Fig. 1C and movie S1). Upon flushing in 1 nM of condensin (*12*) and 5 mM of adenosine triphosphate (ATP), we observed the accumulation of fluorescence density at one spot along the length of the DNA (Fig. 1, D and E, fig. S1, and movie S2). This finding shows that condensin induces local compaction of DNA.

To visualize the compacted DNA structures in the imaging plane of the microscope, we applied flow at a large angle with respect to the double-tethered DNA. This revealed that the bright spots were made up of extended pieces of DNA, consistent with single large DNA loops (Fig. 1, F and G, fig. S2, and movie S3). Importantly, we observed no DNA loop formation by wild-type condensin in the absence of either ATP or Mg^{2+}, when we replaced ATP by the non-hydrolyzable analogs ATPγS or AMPPNP, or when we used a mutant condensin that is unable to bind ATP. Condensin hence creates DNA loops in a strictly ATP-hydrolysis-dependent manner, either by gradually extruding DNA or by randomly grabbing and linking two DNA loci.

To distinguish between these two possibilities, we monitored the looping process by real-time imaging of the DNA while applying constant flow. This revealed the gradual appearance of an initially weak increase in fluorescence intensity at a local spot that grew into an extended loop over time (Fig. 2A, fig. S3, and movies S4 and S5), providing direct visual evidence of loop extrusion and ruling out the random cross-linking model. The extruded loops were in general stable (fig. S4), but occasionally disrupted spontaneously in a single step (Fig. 2A and movie S6). Such a single-step disruption suggests that the DNA loop had been extruded by a single condensin unit that spontaneously let go of the loop, instead of a multi-step relaxation of the loop due to multiple units.

Higher-temporal-resolution imaging allowed us to resolve the two individual DNA strands in the extruded loop in consecutive time frames, which showed that condensin had extruded an actual loop rather than an intertwined, supercoiled, or otherwise connected structure (Fig. 2B, fig. S5, and movie S7).

To quantify the kinetics of loop extrusion, we returned to imaging in the absence of flow. We constructed kymographs from movies where the loop first nucleated as a single weak fluorescent spot that subsequently expanded in size over time (Fig. 3, A and B, and movie S8). We divided each line of the kymograph into the regions outside the loop (I and III) and the DNA loop region itself (II) and calculated, for every frame, the DNA lengths from the fluorescence intensity in each region (Fig. 3C and fig. S6A). This revealed the extrusion of sizeable amounts of DNA into the loop (region II), ranging from 5 kbp to 40 kbp (the upper limit of our assay) before reaching a plateau (fig. S6, B and C). Simultaneously, the DNA content of one of the two outside regions (III) decreased by the same amount, whereas the DNA content of the other outside region (I), surprisingly, did not change at all during the loop-extrusion process (Fig. 3, D to F). This result was consistent in all loop extrusion events that we analyzed quantitatively (N = 36; fig. S6, B to D) and strikingly demonstrates that the loop extrusion process is asymmetric – a finding that is in stark contrast to theoretical loop-extrusion models that have so far been based on two linked motor domains that translocate along the DNA in opposite directions, thereby reeling in DNA symmetrically from both sides (*9–11*).

The asymmetry can be explained if one site in the condensin complex remains stably anchored to the DNA while its motor site translocates along the same DNA. A candidate for such a DNA anchor site is the charged groove formed by the Ycg1 HEAT-repeat and Brn1 kleisin subunits, which entraps DNA by a safety-belt mechanism (*16*). When we repeated the loop-extrusion experiments with a mutant condensin that is unable to fasten the safety belt, the extruded loops no longer remained stable over time, but instead changed size and frequently moved its position (Fig. 3G and fig. S7), resulting in a DNA decrease in one and increase in the other outside region (compare the green curves in Fig. 3, C to G). Furthermore, when we increased the NaCl and Mg^{2+} concentrations of the buffer, we observed unidirectional motion of the extruded loop (fig. S8). The weakening of a stable anchoring point in both experiments is consistent with slippage of DNA through the safety belt. The latter finding also explains the observation of condensin translocation on DNA under the same buffer conditions (*12*).

We can estimate the speed of DNA loop extrusion from the slopes of the initial linear part of the extrusion curves, which yields an average rate of 0.6 kbp/s. As expected, this rate depends on the concentration of ATP (fig. S9) and ATP hydrolysis by condensin (Fig. 3H). Correlation with the end-to-end lengths of individual DNA molecules showed that the speed and efficiency of loop extrusion strongly depended on the relative extension of the DNA, with rates of up to ~1.5 kbp/s and >80% of all DNA molecules displaying loop extrusion at lower DNA extensions (Fig. 3I and fig. S10). Although a direct comparison with Hi-C experiments is impeded by the complexity of chromosomes in cells, it is nevertheless remarkable that condensation rates calculated by this method for condensin II (0.1–0.2 kbp/s) (*17*) or a bacterial SMC complex (0.9 kbp/s) (*18*) are in the same order of magnitude. We note that our assay provides a direct measurement of the condensation rate by individual condensin molecules, since it avoids any discussions about roadblocks, multiple condensin units working in series or in parallel at different positions on the DNA, etc.

The dependence of the extrusion rate on the DNA end-to-end length can be understood as a force dependence: As the loop is extruded, the amount of DNA between the two attachment points (excluding the loop) decreases correspondingly, thus continuously increasing the tension within the DNA (*19*) (to 1.2 ± 0.5 pN; N = 23; see supplementary materials) until the loop-extrusion process stalls (see, for example, Fig. 3D). We used the known force-extension relation for DNA to plot the loop extrusion rate versus force, which revealed a steep dependence on force (Fig. 3J and fig. S11). This very strong force dependence, where the loop extrusion rate drops significantly near 0.4 pN, is consistent with previous magnetic tweezer experiments (*20–22*), which also reported condensation rates that match the loop extrusion rates that we measured at similar forces (Fig. 3J). Together, these findings show that condensin is a fast, yet weak loop-extruding motor that rapidly stalls against a modest force applied to the DNA.

We measured an ATP hydrolysis rate of ~2 molecules per second for condensin in the presence of DNA (fig. S12A). Notably, such a bulk estimate only provides a lower limit of the ATPase activity of condensin complexes in the active loop-extrusion process, since non-DNA-bound condensin molecules and complexes that have stalled on the DNA are included in these assays. If we nevertheless assume, for the sake of argument, that condensin hydrolyzes 2 ATP for extruding ~110 nm (~0.6 kbp) of the folded DNA every second, it would take steps in the order of the 50-nm size of a single condensin complex. Scenarios that explain such large steps must be very different from those for conventional DNA motor proteins that move in single base pair increments (*23*). Models likely need to involve the flexibility of DNA, which allows that, for low forces, condensin can reach nearby spots on the folded DNA to occasionally capture and extrude much longer stretches of DNA than the condensin size

itself (*12*, *24*, *25*). This would be consistent with the very strong force dependence of the extrusion rate that we observe.

Finally, we labeled purified condensin holocomplexes with a single ATTO647N fluorophore (fig. S12) and co-imaged them with SxO-labeled DNA in a Highly Inclined and Laminated Optical (HILO) sheet mode (*26*). As expected, ATTO647N-condensin frequently localized to the stem of the extruded DNA loop (Fig. 4A, fig. S13, and movies S9 and S10). Using real-time monitoring, we consistently observed DNA binding of condensin in a single-step appearance, followed by DNA loop extrusion, and finally single-step bleaching (Fig. 4B and figs. S14 and S15; N = 20). This sequence of events demonstrates that the DNA loop was extruded by a single condensin complex. Kymographs also revealed another class of condensin binding and unbinding events with a short dwell-time that did not lead to DNA loop extrusion (fig. S16A). These were the only DNA-binding events in the absence of ATP (fig. S16B). Furthermore, we observed events where a DNA loop disrupted, while condensin stayed bound to the DNA and later started to extrude a new DNA loop (fig. S14, D and E) – showing that in the process of loop disruption, condensin spontaneously releases the extruded loop rather than dissociates from the DNA.

Quantification of the ATTO647N-condensin intensity provided further evidence that it is a single condensin complex that locates to the stem of the DNA loop: We compared the fluorescence intensity for three cases, (i) condensin binding events that led to DNA loop extrusion, (ii) condensin bleaching events, and (iii) temporary binding events that did not lead to loop extrusion. All three cases revealed the same change in intensity (Fig. 4C), showing that a single condensin complex localizes to the stem of the DNA loop (Fig. 4D). If two condensin complexes would assemble at the loop stem, one would instead have expected a bimodal intensity distribution with two peaks of similar height for single- and double-labeled condensin dimers (based on a 60–85% labeling efficiency, see supplementary materials). Instead, we observed no two-step bleaching events, a majority fraction (33/40) of single-step bleaching events, and a small fraction of DNA molecules (7/40) that showed DNA loop extrusion without any visible fluorescence (fig. S17), as expected for a labeling efficiency of 82%.

Although SMC complexes are vital for chromosome organization in all domains of life, the molecular basis for their action so far remained largely speculative. Our experiments unambiguously demonstrate that condensin exhibits DNA loop-extrusion activity. Our real-time single-molecule dual-color movies of condensin and DNA reveal that loops are extruded by a single condensin complex at the stem of the loop in a manner that is ATP hydrolysis-dependent, strictly asymmetric, and highly sensitive to forces applied to the DNA. These properties can be explained by a model (Fig. 4E) where condensin makes stable contact with DNA at a binding site and then reels in DNA from only one side. The visual proof that condensin is a loop-extruding enzyme reveals the key principle that underlies the organization of genome architecture by condensin and most likely all other SMC protein complexes.

REFERENCES AND NOTES

1. L. Aragon, E. Martinez-Perez, M. Merkenschlager, Condensin, cohesin and the control of chromatin states. *Curr. Opin. Genet. Dev.* **23**, 204–211 (2013). doi:10.1016/j.gde.2012.11.004 Medline

2. F. Uhlmann, SMC complexes: From DNA to chromosomes. *Nat. Rev. Mol. Cell Biol.* **17**, 399–412 (2016). doi:10.1038/nrm.2016.30 Medline

3. K. Jeppsson, T. Kanno, K. Shirahige, C. Sjögren, The maintenance of chromosome structure: Positioning and functioning of SMC complexes. *Nat. Rev. Mol. Cell Biol.* **15**, 601–614 (2014). doi:10.1038/nrm3857 Medline

4. T. Hirano, Condensin-based chromosome organization from bacteria to vertebrates. *Cell* **164**, 847–857 (2016). doi:10.1016/j.cell.2016.01.033 Medline

5. R. Thadani, F. Uhlmann, S. Heeger, Condensin, chromatin crossbarring and chromosome condensation. *Curr. Biol.* **22**, R1012–R1021 (2012). doi:10.1016/j.cub.2012.10.023 Medline

6. K. Nasmyth, Disseminating the genome: Joining, resolving, and separating sister chromatids during mitosis and meiosis. *Annu. Rev. Genet.* **35**, 673–745 (2001). doi:10.1146/annurev.genet.35.102401.091334 Medline

7. J. R. Paulson, U. K. Laemmli, The structure of histone-depleted metaphase chromosomes. *Cell* **12**, 817–828 (1977). doi:10.1016/0092-8674(77)90280-X Medline

8. N. Naumova, M. Imakaev, G. Fudenberg, Y. Zhan, B. R. Lajoie, L. A. Mirny, J. Dekker, Organization of the mitotic chromosome. *Science* **342**, 948–953 (2013). doi:10.1126/science.1236083 Medline

9. A. Goloborodko, M. V. Imakaev, J. F. Marko, L. Mirny, Compaction and segregation of sister chromatids via active loop extrusion. *eLife* **5**, e14864 (2016). doi:10.7554/eLife.14864 Medline

10. E. Alipour, J. F. Marko, Self-organization of domain structures by DNA-loop-extruding enzymes. *Nucleic Acids Res.* **40**, 11202–11212 (2012). doi:10.1093/nar/gks925 Medline

11. A. Goloborodko, J. F. Marko, L. A. Mirny, Chromosome compaction by active loop extrusion. *Biophys. J.* **110**, 2162–2168 (2016). doi:10.1016/j.bpj.2016.02.041 Medline

12. T. Terakawa, S. Bisht, J. M. Eeftens, C. Dekker, C. H. Haering, E. C. Greene, The condensin complex is a mechanochemical motor that translocates along DNA. *Science* **358**, 672–676 (2017). doi:10.1126/science.aan6516 Medline

13. K. Nasmyth, How are DNAs woven into chromosomes? *Science* **358**, 589–590 (2017). doi:10.1126/science.aap8729 Medline

14. M. Ganji, S. H. Kim, J. van der Torre, E. Abbondanzieri, C. Dekker, Intercalation-based single-molecule fluorescence assay to study DNA supercoil dynamics. *Nano Lett.* **16**, 4699–4707 (2016). doi:10.1021/acs.nanolett.6b02213 Medline

15. S. H. Kim, M. Ganji, J. van der Torre, E. Abbondanzieri, C. Dekker, DNA sequence encodes the position of DNA supercoils. bioRxiv 2017/08/24/180414 (2017).

16. M. Kschonsak, F. Merkel, S. Bisht, J. Metz, V. Rybin, M. Hassler, C. H. Haering, Structural basis for a safety-belt mechanism that anchors condensin to chromosomes. *Cell* **171**, 588–600.e24 (2017). doi:10.1016/j.cell.2017.09.008

Medline

17. J. H. Gibcus, K. Samejima, L. Goloborodko, I. Samejima, N. Naumova, J. Nuebler, M. T. Kanemaki, L. Xie, J. R. Paulson, W. C. Earnshaw, L. A. Mirny, J. Dekker, A pathway for mitotic chromosome formation. *Science* **359**, eaao6135 (2018). doi:10.1126/science.aao6135

18. X. Wang, H. B. Brandão, T. B. K. Le, M. T. Laub, D. Z. Rudner, *Bacillus subtilis* SMC complexes juxtapose chromosome arms as they travel from origin to terminus. *Science* **355**, 524–527 (2017). doi:10.1126/science.aai8982 Medline

19. C. Bustamante, S. B. Smith, J. Liphardt, D. Smith, Single-molecule studies of DNA mechanics. *Curr. Opin. Struct. Biol.* **10**, 279–285 (2000). doi:10.1016/S0959-440X(00)00085-3 Medline

20. J. M. Eeftens, S. Bisht, J. Kerssemakers, M. Kschonsak, C. H. Haering, C. Dekker, Real-time detection of condensin-driven DNA compaction reveals a multistep binding mechanism. *EMBO J.* **36**, 3448–3457 (2017). doi:10.15252/embj.201797596 Medline

21. J. Eeftens, C. Dekker, Catching DNA with hoops-biophysical approaches to clarify the mechanism of SMC proteins. *Nat. Struct. Mol. Biol.* **24**, 1012–1020 (2017). doi:10.1038/nsmb.3507 Medline

22. T. R. Strick, T. Kawaguchi, T. Hirano, Real-time detection of single-molecule DNA compaction by condensin I. *Curr. Biol.* **14**, 874–880 (2004). doi:10.1016/j.cub.2004.04.038 Medline

23. W. Yang, Lessons learned from UvrD helicase: Mechanism for directional movement. *Annu. Rev. Biophys.* **39**, 367–385 (2010). doi:10.1146/annurev.biophys.093008.131415 Medline

24. J. Lawrimore, B. Friedman, A. Doshi, K. Bloom, RotoStep: A chromosome dynamics simulator reveals mechanisms of loop extrusion. *Cold Spring Harb. Symp. Quant. Biol.* 10.1101/sqb.2017.82.033696 (2017). doi:10.1101/sqb.2017.82.033696 Medline

25. M.-L. Diebold-Durand, H. Lee, L. B. Ruiz Avila, H. Noh, H.-C. Shin, H. Im, F. P. Bock, F. Bürmann, A. Durand, A. Basfeld, S. Ham, J. Basquin, B.-H. Oh, S. Gruber, Structure of full-length SMC and rearrangements required for chromosome organization. *Mol. Cell* **67**, 334–347.e5 (2017). doi:10.1016/j.molcel.2017.06.010 Medline

26. M. Tokunaga, N. Imamoto, K. Sakata-Sogawa, Highly inclined thin illumination enables clear single-molecule imaging in cells. *Nat. Methods* **5**, 159–161 (2008). doi:10.1038/nmeth1171 Medline

27. J. Yin, A. J. Lin, D. E. Golan, C. T. Walsh, Site-specific protein labeling by Sfp phosphopantetheinyl transferase. *Nat. Protoc.* **1**, 280–285 (2006). doi:10.1038/nprot.2006.43 Medline

28. J. Yin, P. D. Straight, S. M. McLoughlin, Z. Zhou, A. J. Lin, D. E. Golan, N. L. Kelleher, R. Kolter, C. T. Walsh, Genetically encoded short peptide tag for versatile protein labeling by Sfp phosphopantetheinyl transferase. *Proc. Natl. Acad. Sci. U.S.A.* **102**, 15815–15820 (2005). doi:10.1073/pnas.0507705102 Medline

ACKNOWLEDGMENTS

We thank M. Kschonsak for providing the safety-belt mutant condensin complex, J. Kerssemakers and J. van der Torre for technical support, and J. Eeftens, A. Katan, J.-K. Ryu, and E. van der Sluis for discussions. **Funding:** This work was supported by the ERC grants SynDiv 669598 and CondStruct 681365, the Netherlands Organization for Scientific Research (NWO/OCW) as part of the Frontiers of Nanoscience program and a Rubicon Grant, and the European Molecular Biology Laboratory (EMBL). **Author contributions:** M. G. and C. D. designed the single-molecule visualization assay, M. G., E. K., and A. K. performed the imaging experiments, I. A. S. and S. B. developed condensin fluorescence labeling strategies and purified protein complexes, I. A. S. performed ATPase assays, C. D. and C. H. H. supervised the work, M. G., C. H. H., and C. D. wrote the manuscript with input from all authors. **Competing interests:** All authors declare that they have no competing interests. **Data and materials availability:** Original imaging data and protein expression constructs are available upon request.

SUPPLEMENTARY MATERIALS

www.sciencemag.org/cgi/content/full/science.aar7831/DC1
Materials and Methods
Figs. S1 to S17
Movies S1 to S10
References (*27*, *28*)

17 December 2017; accepted 6 February 2018
Published online 22 February 2018
10.1126/science.aar7831

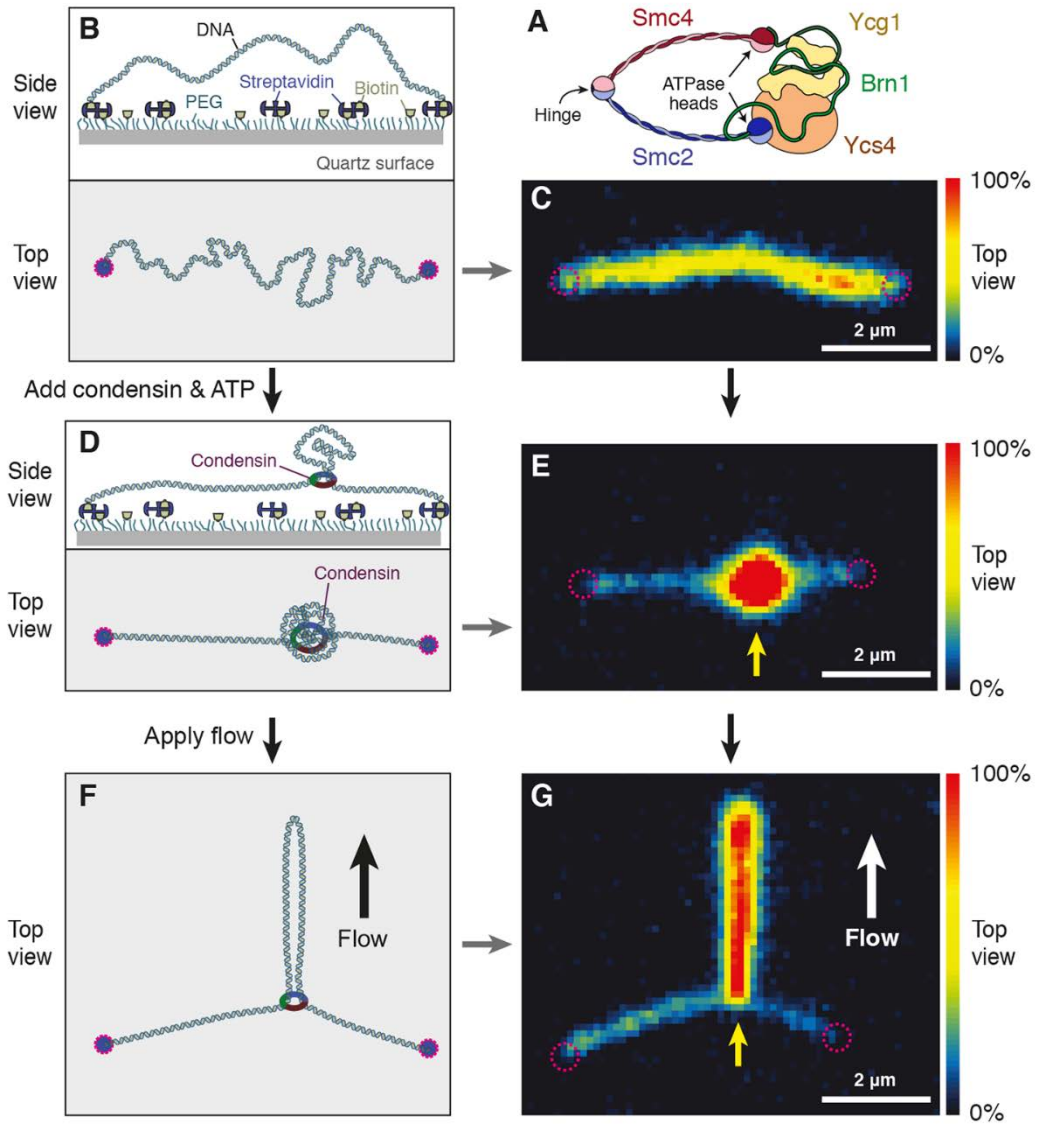

Fig. 1. Single-molecule assay for the visualization of condensin-mediated DNA looping. (**A**) Cartoon representation of the *S. cerevisiae* condensin complex. (**B**) Side and top view schematics of DNA that is doubly tethered to a polyethylene glycol (PEG)-passivated quartz surface via streptavidin-biotin linkage. (**C**) Snap-shot of a double-tethered λ-DNA molecule (100 ms exposure) visualized by Sytox Orange (SxO) staining. Note the homogeneous fluorescence intensity distribution along the DNA. Dashed magenta circles indicate the surface attachment sites of the DNA. (**D**) Side and top view diagrams showing DNA loop formation on double-tethered DNA by condensin. (**E**) Snap-shot of condensin-mediated DNA loop formation at one spot (indicated by the yellow arrow) along a SxO-stained DNA molecule. (**F**) Strategy to visualize DNA loops. Application of flow perpendicular to the axis of the immobilized DNA extends the loop within the imaging plane. (**G**) Snap-shot of an extended DNA loop that is stretched out by flow (white arrow) perpendicular to the DNA, as illustrated in (F).

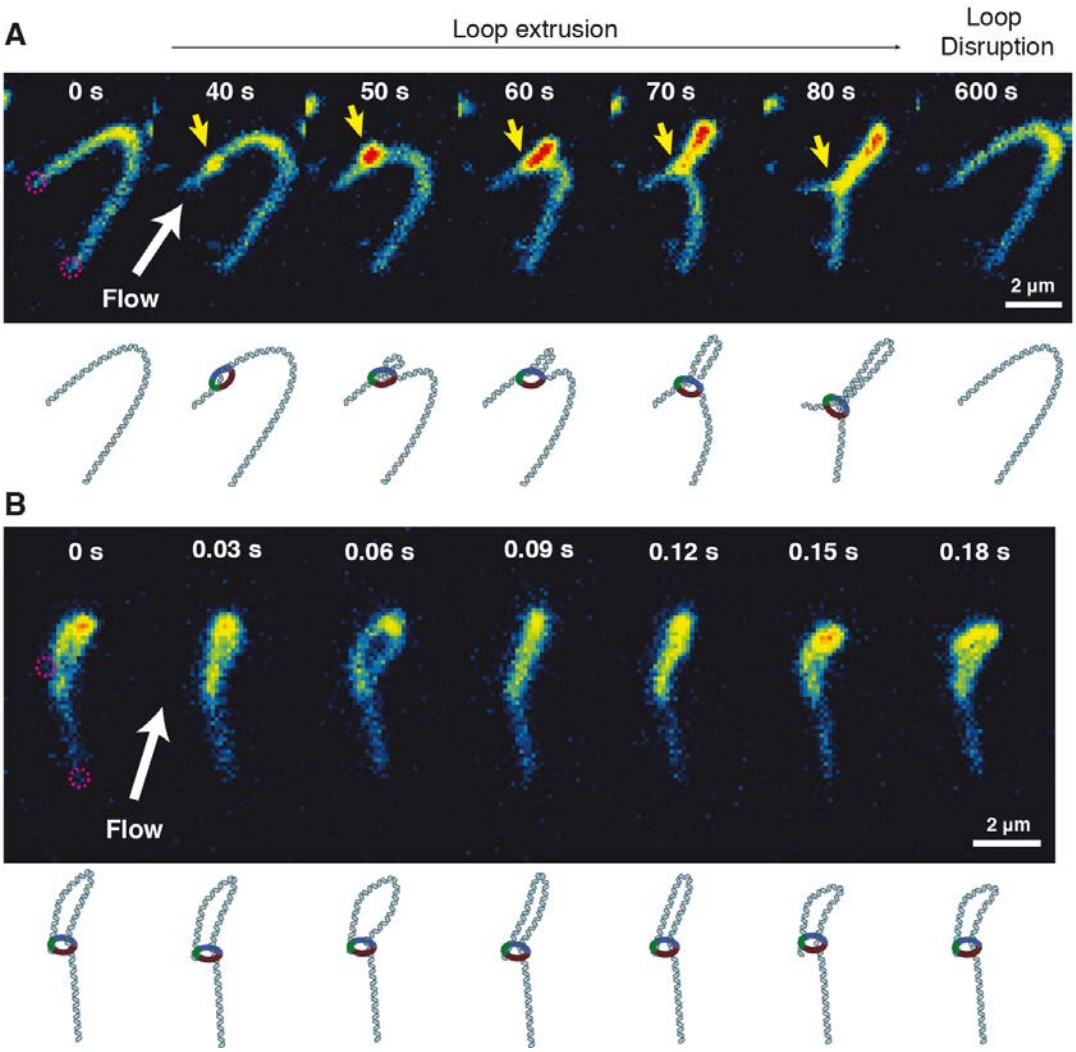

Fig. 2. Real-time imaging of DNA loop extrusion by condensin. (**A**) Series of snap-shots showing DNA loop extrusion intermediates created by condensin on a SxO-stained double-tethered λ-DNA (Movie S3). A constant flow at a large angle to the DNA axis (white arrow) maintains the DNA in the imaging plane and stretches the extruded loop. A yellow arrow indicates the position of the loop base. At ~40 s, a small loop appears that grows over time until ~80 s, consistent with the loop extrusion model. A random linkage model would instead have predicted the sudden appearance of a loop that would have remained stable in size over time. After ~600 s, the loop suddenly disrupted. Schematic diagrams under each snap-shot are for visual guidance. (**B**) High time-resolution imaging reveals the splitting of the two DNA strands in the extruded loop in adjacent time frames.

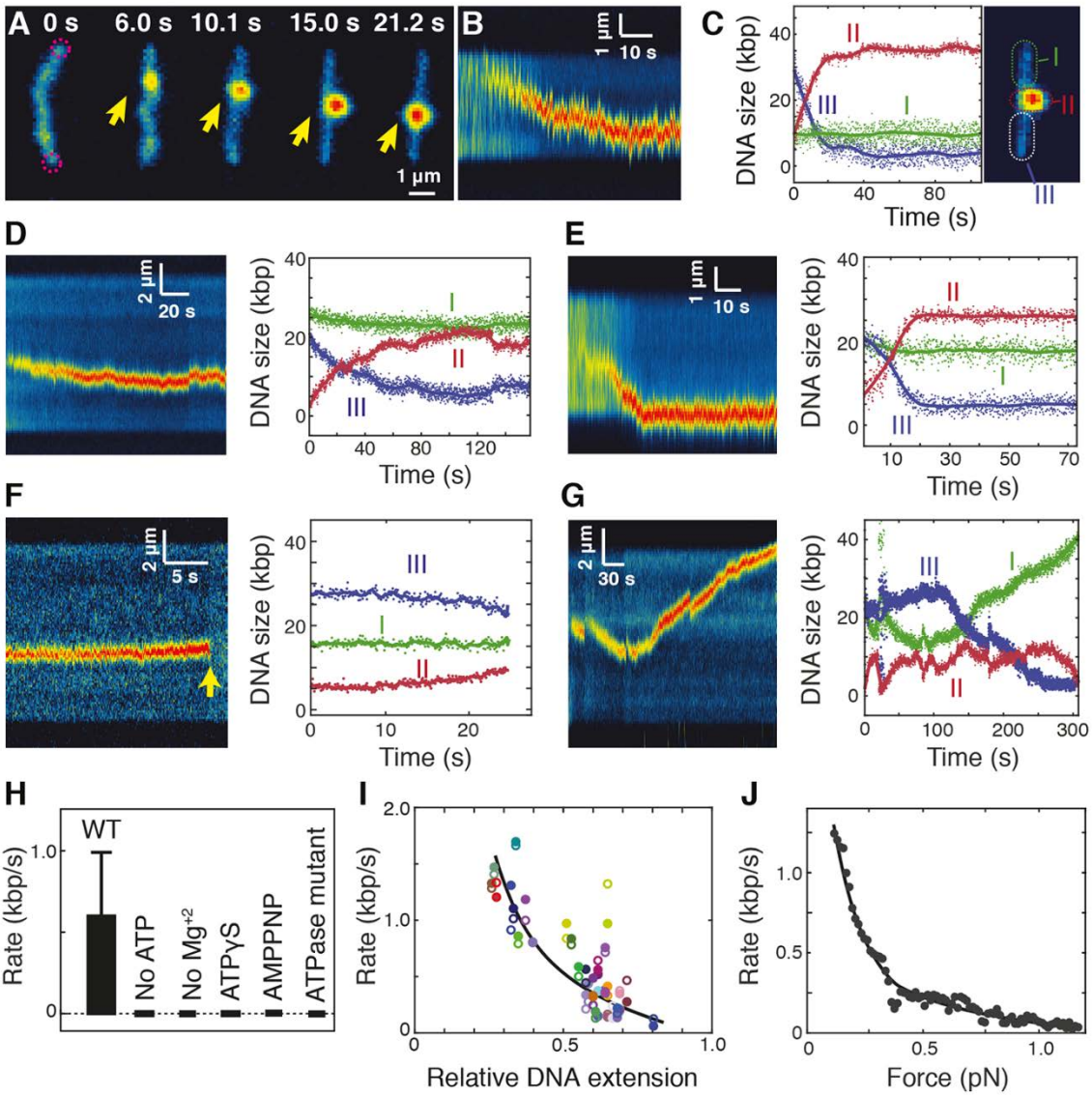

Fig. 3. Loop extrusion is asymmetric and depends on ATP hydrolysis. (**A**) Snap-shots showing the gradual extension of a DNA loop (yellow arrow) on a double-tethered λ-DNA molecule. (**B**) Kymograph of SxO fluorescence intensities shown in (A). (**C**) DNA lengths calculated from the integrated fluorescence intensities and the known 48.5-kbp length of the λ-DNA in the kymograph of panel (B) for regions outside the loop (I and III) and the loop region itself (II). (**D** to **F**) Fluorescence kymographs and intensity plots of a more stretched DNA molecule (end-to-end distance 9.1 µm) where the DNA loop stalls midway (D), of a DNA molecule where loop extrusion starts in the center and continues until reaching the physical barrier at attachment site (E), and of a loop-extrusion event that abruptly disrupts in a single step. (**G**) Kymograph and intensity plot for loop extrusion by a safety-belt condensin mutant complex, which displays dynamic changes of all three DNA regions and of the loop position. (**H**) Average loop extrusion rates (mean±SD) under various conditions. (**I**) Rate of loop extrusion plotted versus the relative DNA extension in relation to its 20-µm contour length. Filled circles are calculated from region II, open circles from region III, the line serves as a visual guide. (**J**) Rate of loop extrusion plotted versus the force exerted within the DNA due to increased DNA stretching upon increase of the loop size. The line serves as a visual guide.

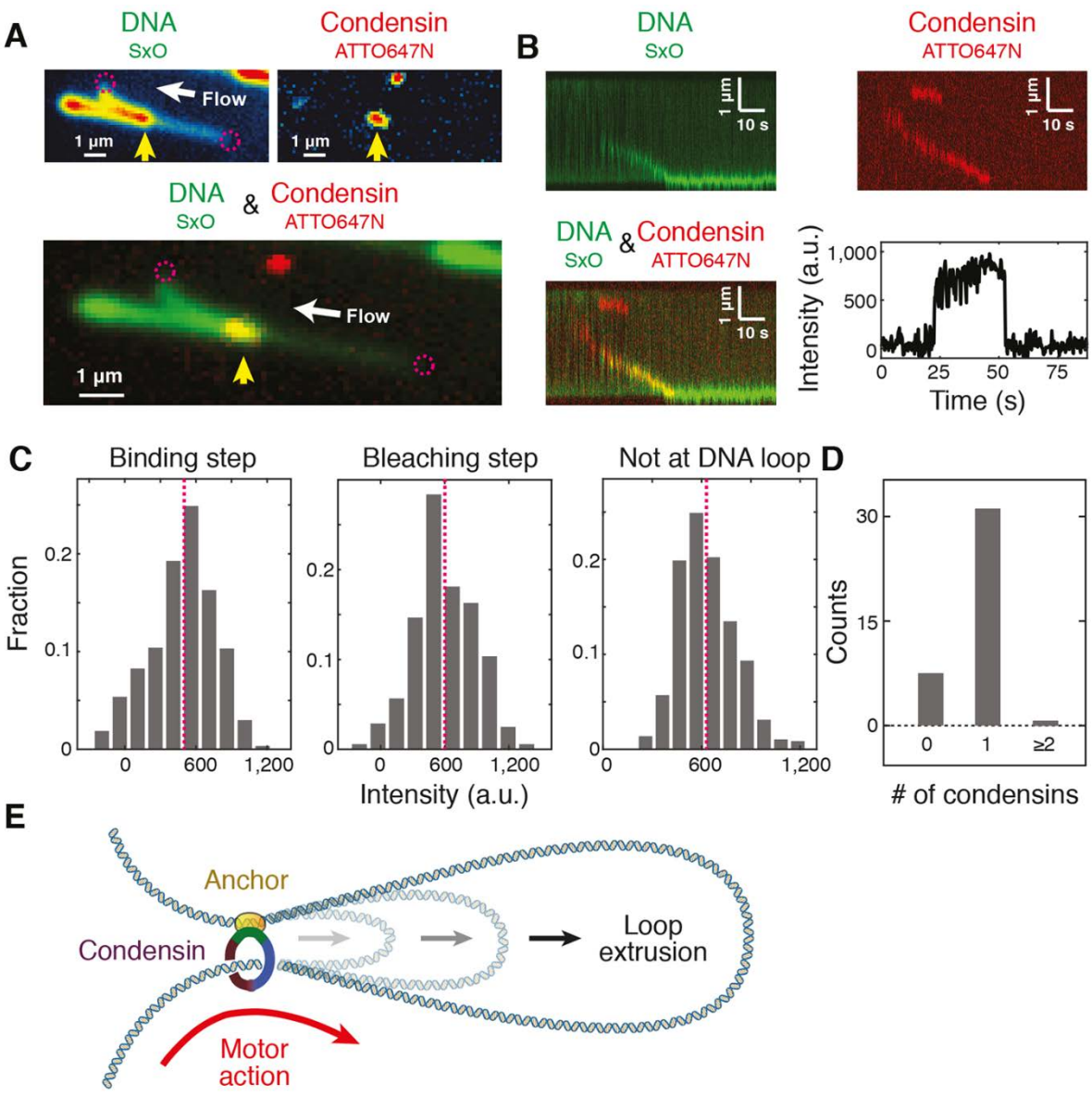

Fig. 4. Loop extrusion is induced by a single condensin complex. (**A**) Images of the same field of view of SxO-stained DNA (top left), ATTO647N-labeled condensin (top right) and their merge (bottom) reveal condensin at the stem of an extruded DNA loop (yellow arrow). Images are integrated over 2 s of a movie. (**B**) Kymographs of SxO-stained DNA (top left), ATTO647N- condensin (top right) and their merge (bottom left) of a real-time movie of DNA loop extrusion. The corresponding ATTO647N fluorescence time trace (bottom right) shows single-step binding and single-step photobleaching events of the DNA-bound condensin. (**C**) Fluorescence intensity distributions for condensin binding events that led to DNA-loop extrusion (left), condensin bleaching in such events (middle), and binding events that did not lead to loop extrusion (right) measured under similar optical conditions. (**D**) Histogram of the number of condensin complexes that show loop extrusion activity as counted from the fluorescence steps. (**E**) Model for DNA loop extrusion by condensin. One strand of DNA is anchored by the kleisin and HEAT-repeat subunits (yellow-orange) of the condensin complex, which extrudes a loop of DNA.

Real-time imaging of DNA loop extrusion by condensin

Mahipal Ganji, Indra A. Shaltiel, Shveta Bisht, Eugene Kim, Ana Kalichava, Christian H. Haering and Cees Dekker

published online February 22, 2018